ENVIRONMENTAL RESEARCH
LETTERS

LETTER • OPEN ACCESS

Observed changes in convective and stratiform precipitation in Northern Eurasia over the last five decades

To cite this article: Alexander Chernokulsky *et al* 2019 *Environ. Res. Lett.* **14** 045001

Environmental Research Letters

LETTER

Observed changes in convective and stratiform precipitation in Northern Eurasia over the last five decades

Alexander Chernokulsky[1,7], **Fedor Kozlov**[1,2], **Olga Zolina**[3,4], **Olga Bulygina**[5], **Igor I Mokhov**[1,2] and **Vladimir A Semenov**[1,6]

[1] A.M. Obukhov Institute of Atmospheric Physics Russian Academy of Sciences, Moscow, Russia
[2] Lomonosov Moscow State University, Moscow, Russia
[3] L'Institut des Géosciences de l'Environnement, Grenoble, France
[4] P.P. Shirshov Institute of Oceanology Russian Academy of Sciences, Moscow, Russia
[5] All-Russian Research Institute of Hydrometeorological Information–World Data Center, Obninsk, Russia
[6] Institute of Geography, Russian Academy of Sciences, Moscow, Russia
[7] Author to whom any correspondence should be addressed.

E-mail: a.chernokulsky@ifaran.ru

OPEN ACCESS

RECEIVED
31 August 2018

REVISED
3 December 2018

ACCEPTED FOR PUBLICATION
2 January 2019

PUBLISHED
20 March 2019

Keywords: precipitation extremes, convective showers, precipitation types, stratiform precipitation, regional climate changes, surface observation

Supplementary material for this article is available online

Abstract

Long-term changes in convective and stratiform precipitation in Northern Eurasia (NE) over the last five decades are estimated. Different types of precipitation are separated according to their genesis using routine meteorological observations of precipitation, weather conditions, and morphological cloud types for the period 1966–2016. From an initial 538 stations, the main analysis is performed for 326 stations that have no gaps and meet criteria regarding the artificial discontinuity absence in the data. A moderate increase in total precipitation over the analyzed period is accompanied by a relatively strong growth of convective precipitation and a concurrent decrease in stratiform precipitation. Convective and stratiform precipitation totals, precipitation intensity and heavy precipitation sums depict major changes in summer, while the relative contribution of the two precipitation types to the total precipitation (including the contribution of heavy rain events) show the strongest trends in transition seasons. The contribution of heavy convective showers to the total precipitation increases with the statistically significant trend of 1%–2% per decade in vast NE regions, reaching 5% per decade at a number of stations. The largest increase is found over the southern Far East region, mostly because of positive changes in convective precipitation intensity with a linear trend of more than 1 mm/day/decade, implying a 13.8% increase per 1 °C warming. In general, stratiform precipitation decreases over the majority of NE regions in all seasons except for winter. This decrease happens at slower rates in comparison to the convective precipitation changes. The overall changes in the character of precipitation over the majority of NE regions are characterized by a redistribution of precipitation types toward more heavy showers.

1. Introduction

A considerable threat to society from the observed global climate change comes from the changes in precipitation characteristics. In Northern Eurasia (NE), increasing precipitation intensities and the occurrence of heavy rain events (Semenov and Bengtsson 2002, Groisman *et al* 2005, Mokhov *et al* 2005, Ye *et al* 2015, Donat *et al* 2016, Zolina and Bulygina 2016), and changes in the duration of wet and dry spells (Khon *et al* 2007, Zolina *et al* 2010, 2013, Ye 2018), affect national economies by modulating streamflow and water availability (Mokhov *et al* 2003, Milly *et al* 2005, Shkolnik *et al* 2018) and causing local devastating flashfloods (Meredith *et al* 2015b) or large-scale deluges (Mokhov 2014, Mokhov and Semenov 2016).

A careful look at the structural changes in precipitation is required in order to understand the observed tendencies and estimate future changes (Groisman *et al* 1999). Whereas in the climate models distinguishing between stratiform and convective precipitation is straightforward, as they are simulated as different variables, separating these precipitation types in the real world is challenging (Houze 1997) and requires an analysis of supplementary weather parameters. This problem is the focus of ongoing large environmental and climate dynamics regional initiatives (Groisman *et al* 2017, Collins *et al* 2018).

Global climate change may impact the static stability of the troposphere. In particular, a significant increase of the tropospheric lapse rate was found over NE and Europe in the second half of the 20th century (Mokhov and Akperov 2006) with the possible intensification of convective processes. An indication of such a tendency is the increase of convective cloud cover (Sun *et al* 2001, Chernokulsky *et al* 2011, 2017a) and convective instability indices (Riemann-Campe *et al* 2009, Pistotnik *et al* 2017) over NE, which may lead to the more frequent formation of severe convective events (Kurgansky *et al* 2013, Chernokulsky *et al* 2017b, Taszarek *et al* 2018). Favorable conditions for severe convective events may become more frequent over the course of the 21st century, according to climate model projections (Marsh *et al* 2009, Púčik *et al* 2017, Chernokulsky *et al* 2017b).

Intensification of convective processes may increase the contribution of convective rainfall to the total precipitation. Recent studies show an increase in the convective precipitation in central Europe (Rulfová and Kyselý 2014) and NE (Han *et al* 2016, Ye *et al* 2017), which could be a consequcne of the warming (Berg *et al* 2013, Ye *et al* 2016, Peleg *et al* 2018). In particular, Ye *et al* (2017) found a very strong increase in convective precipitation (with the trend in the annual total being of 36.7 mm/decade and sensitivity to temperature amounting to 18% $^{\circ}C^{-1}$) accompanied by a simultaneous decrease of stratiform precipitation for the 1966–2000 period. However, many of these trends should be treated with caution due to the impact of abrupt step-like discontinuities in three-hourly observation records for clouds (Eastman and Warren 2013) and corresponding weather character.

In this paper, we separately analyze changes in the convective and stratiform precipitation for the 1966–2016 period using routine meteorological observations of precipitation, present and past weather, and morphological cloud types to classify the two precipitation types. We demonstrate that for this longer period an observed increase in the total precipitation intensity is also associated with an increase in convective rainfall intensity and a growing contribution of heavy and intense showers. However, the increase in convective precipitation is smaller compared to that reported previously due to the exclusion of station data exhibiting artificial changes and, to a lesser degree, due to choosing a longer period.

2. Data and methods

2.1. Discriminating between different types of precipitation by their genesis

Various approaches have been proposed to discriminate between convective (solely thermodynamic driven) and stratiform (dynamic driven) precipitation. Some approaches reveal the type of precipitation by establishing thresholds for precipitation characteristics and associated measures (for instance, radar reflectivity, rain intensity, cloud drop size, ice and liquid water paths, graupel presence, etc), which can be measured using remote sensing by radars, satellites, and optical disdrometers (see e.g. Alibegova 1985, Steiner and Smith 1998, Sempere-Torres *et al* 2000, Anagnostou 2006, Sui *et al* 2007, Xu *et al* 2013, Yang *et al* 2013, Ahmed and Schumacher 2015). Other methods differentiate between convective and stratiform precipitation by analyzing their spatio-temporal structure (Tremblay 2005, Ruiz-Leo *et al* 2013, Han *et al* 2016). The third approach is to use information from routine meteorological observations of weather (present only, or present and past) and/or cloud morphological types. Within this approach, showers and thunderstorms (nonshowery rainfalls and snowfalls) can be attributed to convective (stratiform) precipitation (Evseev 1958, Dai 2001, Berg *et al* 2013, Rulfová and Kyselý 2013, Ye *et al* 2016, Chernokulsky *et al* 2018). Because observations of weather and clouds are synchronized with precipitation observations and have the same time coverage, the approach can be used for estimating decadal variability of different precipitation types (Rulfová and Kyselý 2014, Ye *et al* 2017).

Here, we have utilized routine observations from 538 Russian meteorological stations, collected at the All-Russian Research Institute of Hydrometeorological Information—World Data Center (RIHMI-WDC) for the 1966–2016 period (Bulygina *et al* 2014). We used data on present and past weather (three-hourly observations), cloud morphological types (three-hourly) and precipitation rate (twelve-hourly). Until 1986, precipitation at Russian meteorological stations was measured four-times-a-day (evenly, every six hours, or unevenly, at 3-9-3-9 h, depending on the station). To maintain the temporal homogeneity of data series, we recalculated these earlier four-times-a-day observations to two-times-a-day ones (with 12 h interval). Furthermore, through the comparison with the existing RIHMI-WDC datasets on daily and monthly precipitation rates, we corrected 700 records in the initial dataset that were erroneous due to digitizing mistakes during the manual transfer of information from punch cards for the 1960–1980 period (e.g. a 12.2 mm value was digitized as

a 102.2 mm value) (see Chernokulsky *et al* 2018 for more details).

To discriminate among different types of precipitation (specifically, showery, nonshowery, and drizzle), we used codes of present and past weather and information on cloud morphological types that were recorded concurrently with the precipitation report and for three preceding reports (equivalent to 12 h) (Chernokulsky *et al* 2018). We used information on present weather as the primary criterion (82% of precipitation reports were assigned to a particular type using this criterion), past weather as the second priority criterion (16.5%) and morphological cloud types as the third priority criterion (1.5%). In other words, if a code (or codes) of present weather was attributed to a convective event (in particular, WMO codes 13, 17–19, 25–27, 29, 80–99) (see, for details, Dai 2001, Chernokulsky *et al* 2018) the precipitation report was considered as showery. If four codes of present weather were not associated with a particular precipitation type, then the past weather codes were checked. If they also failed to separate precipitation type, then information on clouds was used to finally provide attribution. Nonshowery and drizzle precipitation were identified in a similar way (see supplementary figure S1, available online at stacks.iop.org/ERL/14/045001/mmedia, for more details). Occasionally, codes of various precipitation types may occur over 12 h; it this case, the corresponding precipitation value is considered as compound. If none of the criteria unambiguously defined the precipitation type, the related rainfall event was marked as undefined.

Utilizing information on both past and present weather together with information on cloud types and using 12 h precipitation data (instead of daily) we are capable of substantially reducing the number of reports with compound and undefined precipitation (down to 9.2% and 0.9% of all reports, respectively). In particular, the number of reports with compound precipitation is half that estimated by Ye *et al* (2017).

2.2. Exclusion of stations with erroneous reports

The accuracy of the proposed method depends on the homogeneity of standard weather observations that are uniform for various seasons, various regions, and various temporal periods (at least for the examined period 1966–2016, when the observation procedure has not been changed). This allows us to restore consistent values of different precipitation types in space and time. Inherent uncertainties of the method are associated with the peculiarities of the weather observing procedure and practices, such as the restriction of the visible horizon, difficulty of embedded convection determination, coding specifications and some other issues (see Chernokulsky *et al* 2018 for more details). These uncertainties may alter the retrieval of precipitation characteristics, but their impact is largely of a random nature and has a minor effect on trend estimates. The method is also sensitive to the training of observers. Thus, a well trained observer being replaced by a poorly trained one may apparently result in the appearance of inhomogeneity in time series. Such time series (if any) should be excluded from the analysis.

When examining variations of cloud types worldwide, Eastman and Warren (2013) revealed an artifact-like character of instant reversal in time series of the cumulonimbus and nimbostratus cloud amount for many Russian meteorological stations. Since the observed weather and cloud types are inherently related, the corresponding artifact-like changes can be found in present weather code time series. Indeed, an inspection of time series with the frequencies of reports that were associated with particular precipitation types revealed the presence of such artificial reversals for several stations (figure S2) (with the absence of such changes at the neighboring stations). The nature of these local instant reversals is still unclear. They are not linked to the station location or year of changes. Because reversals had occurred in different years, they tend to be masked when the regional analysis based on the aggregation of many stations is performed. We assumed that these abrupt changes were associated with a change of observer; but confirmation was not possible due to the lack of metadata.

To eliminate problematic stations from further analysis, we applied a step-testing procedure similar to one used by Eastman and Warren (2013). At the beginning, discontinuity was taken as the maximum of the time derivative of the five-year running mean of the ratio between showery reports and all precipitation-weather reports. Further, significance of abrupt change was tested by comparing the samples of the ratio between the preceding and subsequent (with respect to the break) values in two ways. First, the two means were verified for overlapping (within their standard deviations) (as in Eastman and Warren 2013). Second, the nonparametric Mann–Whitney U-test for the comparison of two sample means was carried out. We performed further analysis only for the stations where the before-reversal and after-reversal means overlapped or (and) two samples passed the U-test (at the significant level of 0.05).

In addition, we restricted our consideration to records for which the number of totally missing years was less than five years (we considered the whole year to be missing if data for any day of the year was missing) and to the stations with an elevation of below 1000 m. We also excluded all stations that had been relocated during the analyzed period. In total, 111 stations were omitted. From the remaining 427 stations, we excluded an additional 101 stations because they failed to pass both tests on the artificial instant reversal insignificance. Finally, 326 stations in total (with 154 passing one of the tests, and 172 passing both) were selected for the analysis (figure 1).

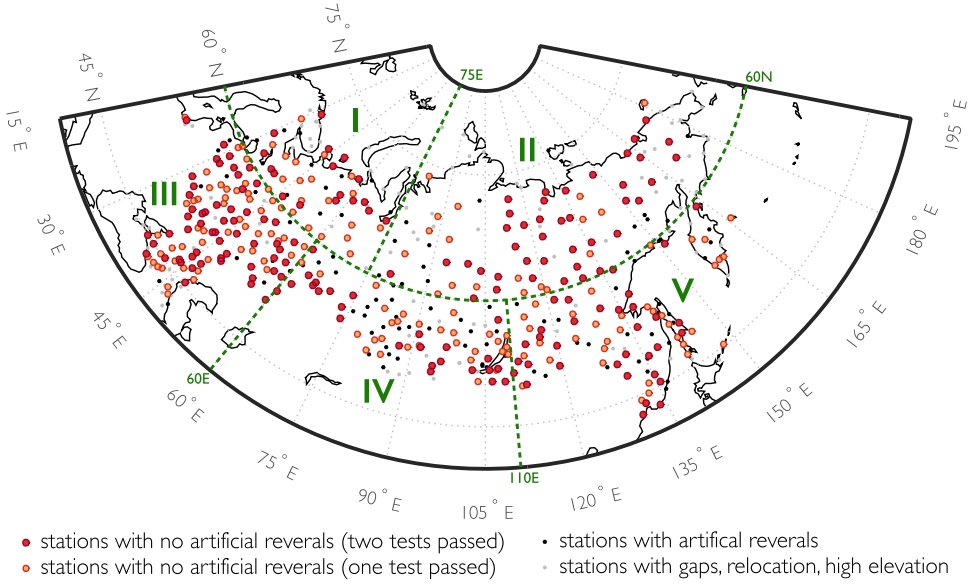

Figure 1. Location of Russian meteorological stations from RIHMI-WDC dataset. Stations that have gaps of ⩾5 years, had been relocated, or have elevation ⩾1000 m are shown with small grey dots. Stations that failed to pass tests on artificial instant reversal absence are shown with black circles. Orange (red) circles denote stations that passed only one (both) test(s). Green dashed lines show the division into five regions (I—northern European part (north of 60 N, west of 75E), II—northern Asian part (north of 60 N, east of 75E), III—southern European part (south of 60 N, west of 60E), IV—southern Siberia (south of 60 N, between 60E and 110E), V—southern Far East (south of 60 N, east of 110E)).

2.3. Precipitation characteristics

We analyzed the seasonal/annual precipitation totals P (in mm), frequency of precipitation events pP (fraction of wet days over a season/year), and precipitation intensity I (precipitation total scaled by the number of wet days, in mm/day). We also evaluated the precipitation accumulated during very wet days (>95th percentile, which is obtained from empirical distribution for each station for the whole period) ($P95$, in mm) and its contribution to precipitation totals ($R95p = 100 \cdot P95/P$, in %) (Klein Tank and Konnen 2003). All values were counted for both convective and stratiform precipitation and were denoted by subscripts 'Conv' and 'Strat', respectively (for example, $R95p_{\mathrm{Conv}} = P95_{\mathrm{Conv}}/P_{\mathrm{Conv}}$). The variable without the subscript stands for the characteristic of total precipitation (sum of all types). In addition, we calculated the fraction of P_{Conv} and P_{Strat} in the total precipitation P (f_{Conv} and f_{Strat} respectively; thus, $f_{\mathrm{Conv}} = 100 \cdot P_{\mathrm{Conv}}/P$, in %) and the contribution of $P95_{\mathrm{Conv}}$ and $P95_{\mathrm{Strat}}$ to P ($R95pTOT_{\mathrm{Conv}}$ and $R95pTOT_{\mathrm{Strat}}$, respectively; thus, $R95pTOT_{\mathrm{Conv}} = 100 \cdot P95_{\mathrm{Conv}}/P$, in %). We note that the results related to $R95p$ and $R95pTOT$ indices should be treated with caution due to a finite number of wet days per season (it is even more restricted for various precipitation types) (Zolina *et al* 2009, Leander *et al* 2014, Schär *et al* 2016).

We estimated linear trends of the aforementioned precipitation characteristics for each station separately and for five regions (where all stations were simply averaged with equal weight) (region boundaries are shown in figure 1). We used a nonparametric linear Theil–Sen slope estimator (which is less sensitive to outliers than standard linear regression, it is of particular importance for estimating $R95p$ and $R95pTOT$ trends) to calculate the trend slope, and a nonparametric Mann–Kendall test to estimate the significance of the trend. To estimate whether the trend (of either sign) pattern holds field (or group) significance (i.e. the conclusion about growing/declining tendency can be attributed to the considered domain), we calculated the field significance of the trend patterns. The analysis was performed, according to Livezey and Chen (1983), using binominal distribution and with the assumption that all individual trend estimates are independent.

3. Results

Total precipitation P has experienced a moderate increase over the NE region over the last five decades (figure 2) (see also Bogdanova *et al* 2010). The most pronounced statistically significant trends are found in the south of the Far East (figure 2(a)) which is in concordance with previously obtained results (e.g. Groisman *et al* 2014). The opposite trends of annual P_{Conv} and P_{Strat} (increase and decrease, respectively) are significant for the majority of stations. Absolute magnitudes of the trends exceed 50 mm/decade for several regions (figures 2(b), (c)). The major increase of P_{Conv} occurs at Sakhalin Island (up to 120 mm/decade), while P_{Strat} is reduced dramatically at the lower basin of the Amur River (down to –76 mm/decade). Similar magnitudes of P_{Conv} and P_{Strat} trends were found by Ye *et al* (2017) for a shorter period (up to 2000), but in the south of Siberia. Note that very few stations display reverse trends (decrease of P_{Conv} and increase of P_{Strat}). Several

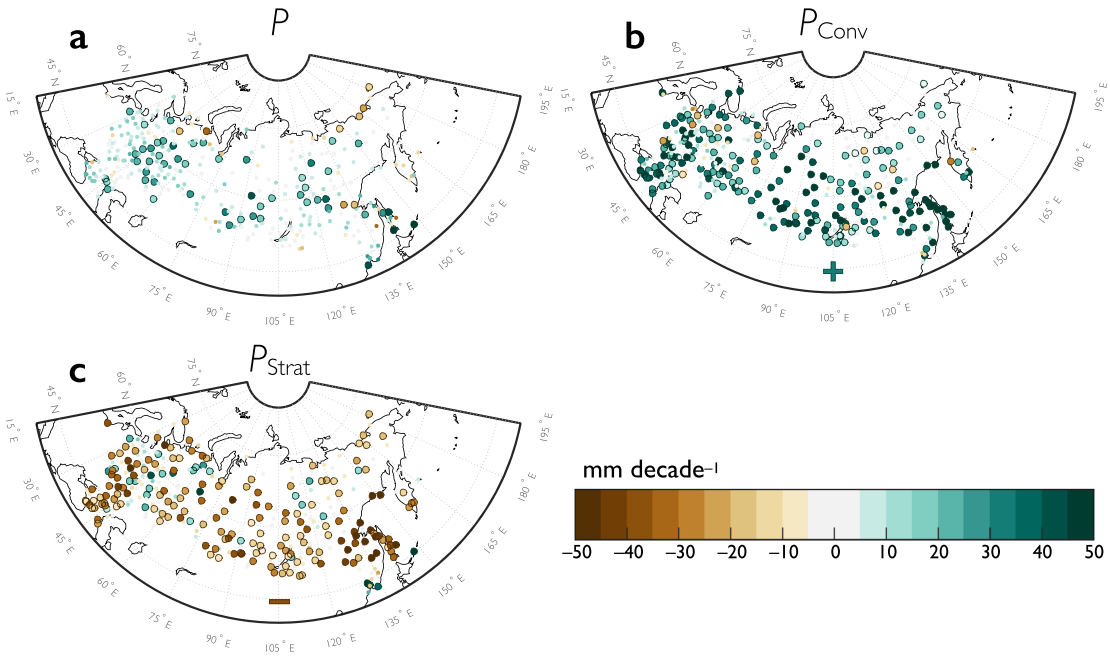

Figure 2. Trends (obtained with the nonparametric Theil–Sen estimator) for annual total precipitation totals P (a), convective precipitation totals P_{Conv} (b), and stratiform precipitation totals P_{Strat} (c) for the 1966–2016 period. Trends are shown only for 326 stations that passed at least one of the tests on artificial instant reversal absence. Large circles stand for statistical significant trends. Significance is computed with the nonparametric Mann–Kendall test (at 0.05 significant level). Plus and minus signs denote the entire NE patterns that holds field significance (at 0.1 significance level).

seasonal peculiarities of P_{Conv} and P_{Strat} changes are revealed (figure 3). In winter, positive trends for P_{Strat} are found at stations in the European part of Russia (up to 17 mm/decade) (figure 3(b)). The strongest decline in P_{Strat} occurs in the Far East regions in summer (down to –25 mm/decade) and autumn (down to –26 mm/decade) (figures 3(f), (h)). It is collocated with the P_{Conv} increase in this region in the same seasons (up to 40 mm/decade) (figures 3(e), (g)). For the European part, the highest rates of the seasonal P_{Conv} trend are revealed in spring (the absolute maximum is found in Sochi with 28 mm/decade) (figure 3(c)). In general, the increase of P_{Conv} and the decrease of P_{Strat} happen in different seasons. Specifically, the largest number of stations exhibit significant positive P_{Conv} trends in spring and autumn, while the largest number of stations show significant negative P_{Strat} trends for summer. A more pronounced increase in convective clouds occurrence in transition seasons than in summer was revealed previously in Northern Eurasia and North America by Sun *et al* (2001). They associated it with the 'saturation' of summer seasons with convective event frequency, while unsaturated spring and autumn become more 'summer-like' seasons, which is partly confirmed by the obtained tendencies of precipitation (see also Ye *et al* 2016).

Changes in f_{Conv} and f_{Strat} (figure S3) reflect the joint effect of changes in P_{Conv} and P_{Strat} and are linked to the absolute values of P. Thus, maximum trends of f_{Conv} and f_{Strat} are revealed in winter when P is relatively small (close to 20%/decade for several stations, which means almost an entire replacement of stratiform by convective precipitation). For annual means, f_{Conv} and f_{Strat} have significant trends within 2%–15%/decade.

Similar tendencies are obtained for the frequency of convective and stratiform precipitation (pP_{Conv} and pP_{Strat}) (figure S4). For annual means, the majority of stations display a pP_{Conv} increase (up to 0.06/decade) and pP_{Strat} decline (down to –0.03/decade) with generally higher values in southern regions and lower in northern regions of NE. Similar tendencies for pP_{Conv} and pP_{Strat} are obtained for seasons. Opposite tendencies are also revealed. Thus, positive trends of pP_{Strat} are common for winter, while negative trends of pP_{Conv} are found in summer (almost a third of stations show a significant decrease in pP_{Conv}).

Changes in P and pP determine variations in daily precipitation intensity I (increase in P and decrease in pP both tend to increase I). On an annual basis (figures 4(a), (b)), the growth of P_{Conv} is more prominent than that of pP_{Conv}, which results in a general increase in I_{Conv} (especially evident over the Far East regions, where I_{Conv} trends are up to 1.4 mm/day/decade). Positive I_{Conv} trends are found in all seasons (figures 4(c), (e), (g), (i)), with the highest increase in the Far East region (up to 1.8 mm/day/decade for several stations in summer). Decreasing P_{Strat} dominates over decreasing pP_{Strat} on an annual basis in some southern regions (especially over the Okhotsk and Black Sea coasts, where I_{Strat} trends amount to –1.0 mm/day/decade). In the northern part of NE (and in the south of Ural) annual means of I_{Strat} tend to increase (with trends up to 0.5 mm/day/decade). Positive seasonal trends of I_{Strat} are found in the most regions of NE in winter (figure 4(d)) and in some

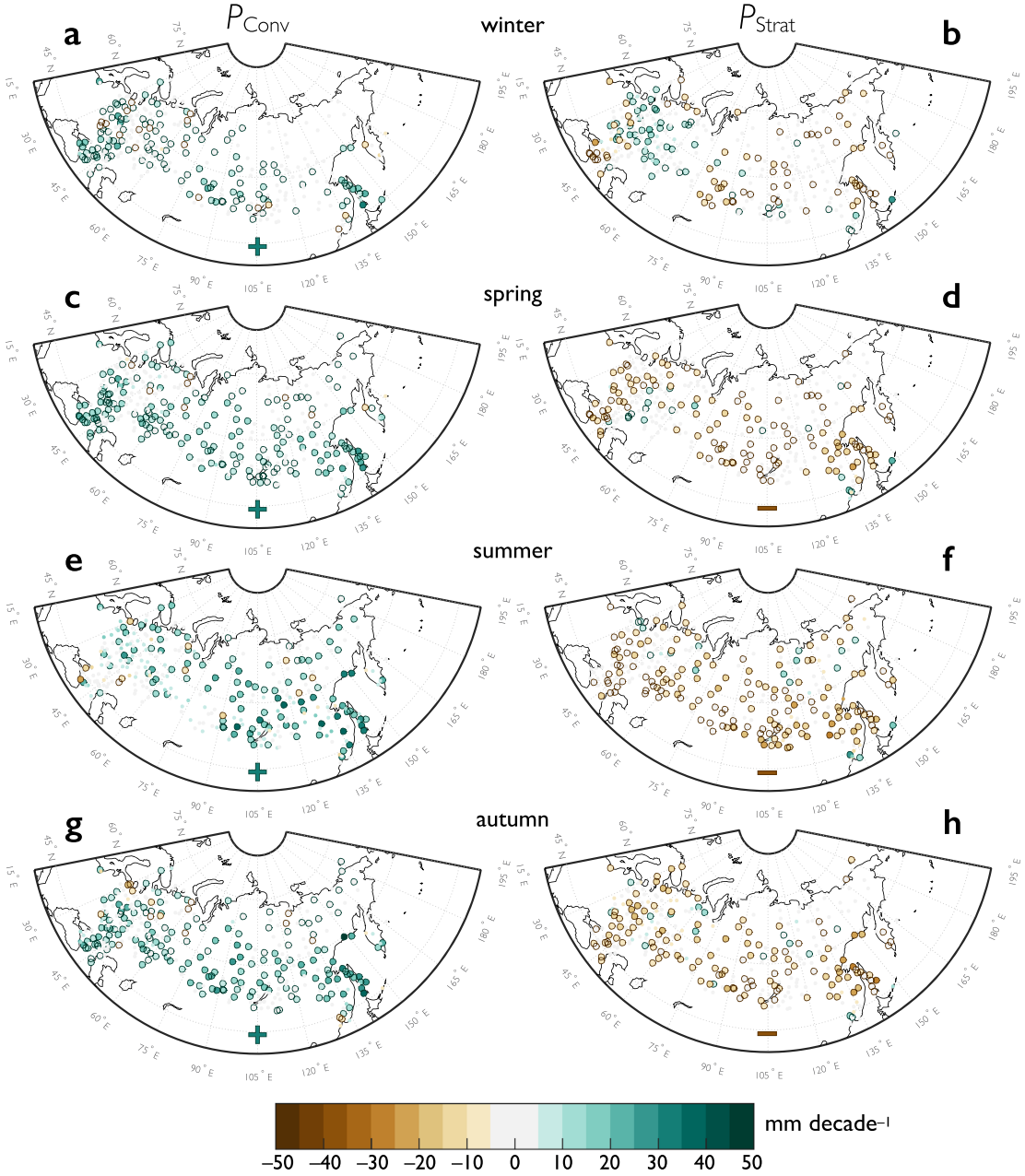

Figure 3. The same as for figure 3, but for winter (a), (b), spring (c), (d), summer (e), (f), and autumn (g), (h) totals of convective precipitation P_{Conv} (a), (c), (e), (g) and stratiform precipitation P_{Strat} (b), (d), (f), (h).

regions in spring (figure 4(f)) and summer (figure 4(h)). The largest I_{Strat} decrease is found at southern stations in summer (with the absolute minimum of –1.87 mm/day/decade in the city of Blagoveshchensk).

Positive P_{Conv} trends and negative P_{Strat} trends are accompanied by same-sign tendencies of heavy precipitation events, specifically, the increase of $P95_{Conv}$ and decrease of $P95_{Strat}$ (figure S5). A significant positive trend of annual $P95_{Conv}$ was obtained for most of the stations (with the maximum value of 52 mm/decade for Nevelsk station at Sakhalin Island). A significant increase of $P95_{Conv}$ is found from spring through autumn. The annual $P95_{Strat}$ tends to decline (with the negative trend down to –30 mm/decade), while changes of seasonal $P95_{Strat}$ are mostly insignificant. Changes in the contribution of heavy precipitation to totals of related precipitation type ($R95p$) are more pronounced for stratiform precipitation. The annual $R95p_{Strat}$ shows a negative trend with the strongest decrease of –10%/decade for several stations in the south of Siberia (figure S6). The largest significant positive trends of annual $R95p_{Conv}$ are found for Sakhalin Island (up to 8%/decade). Seasonal trends of $R95p_{Conv}$ and $R95p_{Strat}$ are generally insignificant (rare heavy precipitation events are often treated as outliers by the Mann–Kendall test and Theil–Sen estimator).

Heavy convective showers tend to contribute more to total precipitation, whereas a portion of heavy stratiform rainfalls in the total precipitation is declining over the analyzed period. That is, changes in

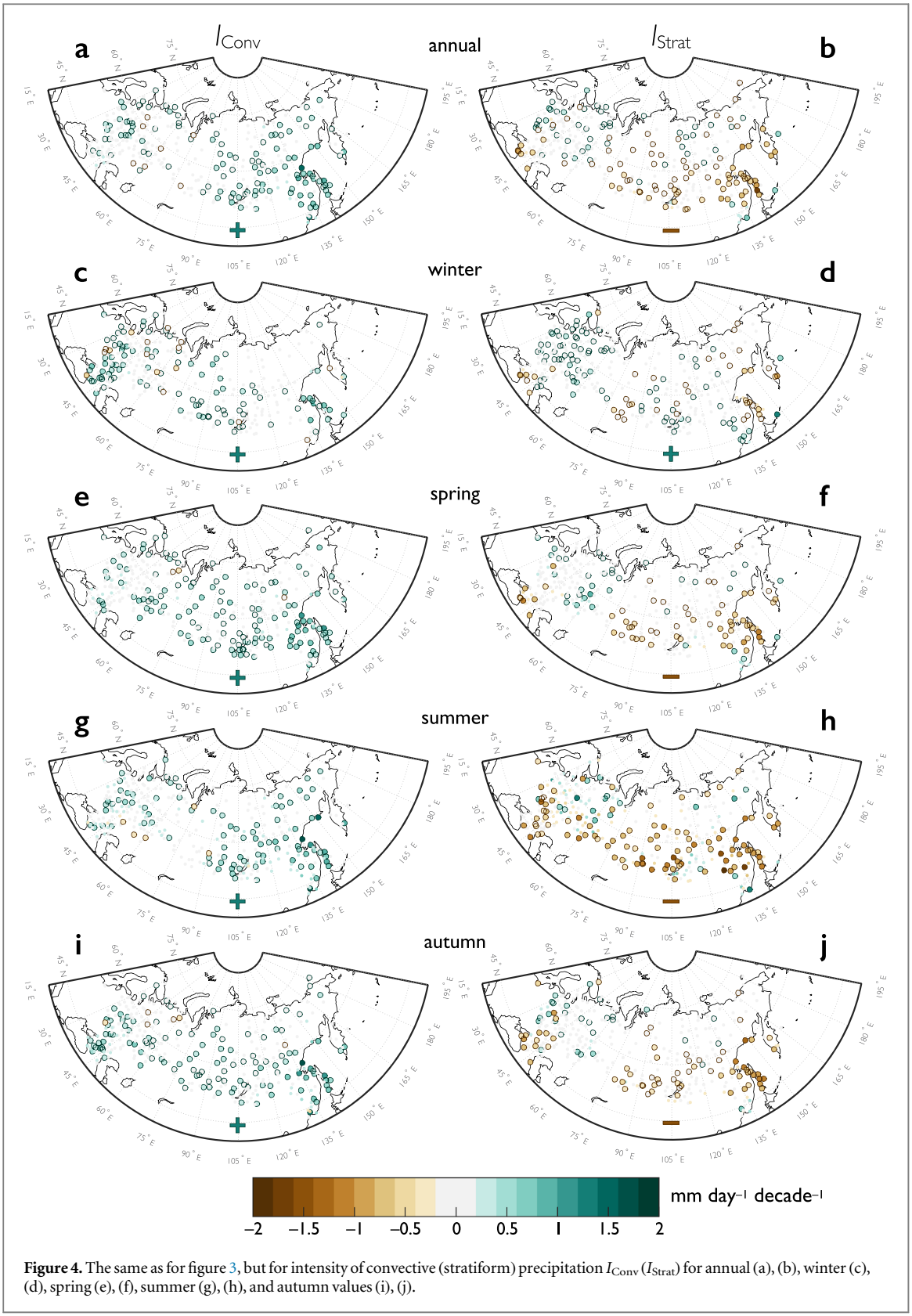

Figure 4. The same as for figure 3, but for intensity of convective (stratiform) precipitation I_{Conv} (I_{Strat}) for annual (a), (b), winter (c), (d), spring (e), (f), summer (g), (h), and autumn values (i), (j).

$R95pTOT_{Conv}$ and $R95pTOT_{Strat}$ are in general concordance with $P95_{Conv}$ and $P95_{Strat}$ changes. Significant positive annual trends of $R95pTOT_{Conv}$ are revealed for many stations with the slopes up to 5%/decade in the south of Siberia and the Far East (figure 5(a)). Changes in $R95pTOT_{Strat}$ are negative with the largest decrease in the central and northern Far East (significant negative trends amount to –6%/decade) (figure 5(b)). Seasonal trends (figures 5(c)–(j)) are significant for a fewer number of stations due to the rarity of heavy precipitation events. The $R95pTOT_{Conv}$ index markedly increases for the warm period of a year (with the maximum trend in summer of 7.1%/decade in the center of the European part of Russia). $R95pTOT_{Strat}$

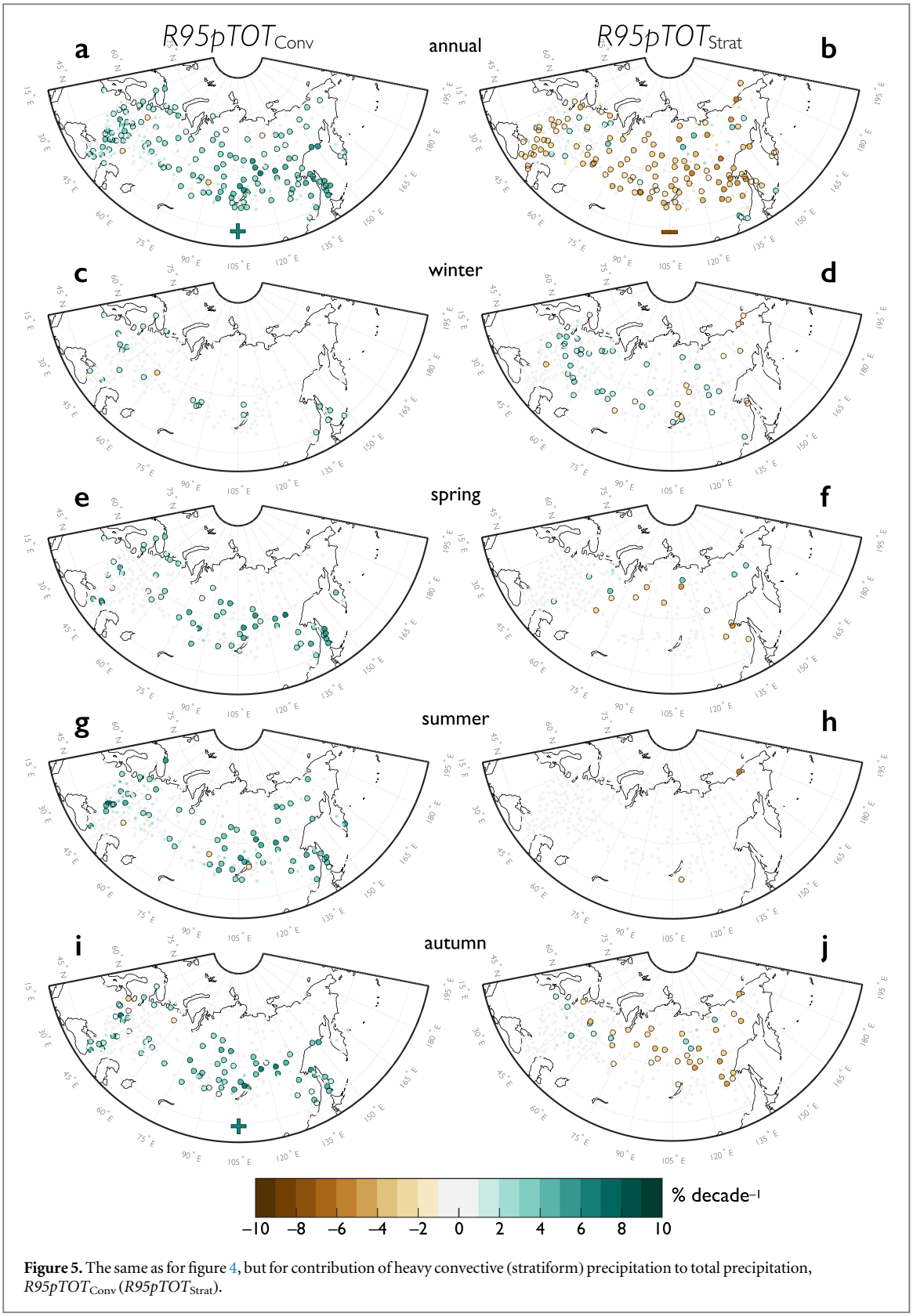

Figure 5. The same as for figure 4, but for contribution of heavy convective (stratiform) precipitation to total precipitation, $R95pTOT_{Conv}$ ($R95pTOT_{Strat}$).

noticeably decreases only in autumn (down to –4.5%/decade), while in winter, significant positive trends are also found (up to 5%/decade for several stations).

Of particular interest is the variability and trends of different precipitation type characteristics aggregated over large regions. Figure 6 shows the long-term variability of annual precipitation totals for five regions (see figure 1 for specification of regions) that were obtained by averaging over all stations in the regions and using only stations that passed tests on artificial instant reversal insignificance. Table 1 summarizes corresponding trend estimates. An elimination of problematic stations with data discontinuities substantially (more than twice for some regions) reduces the magnitude of positive

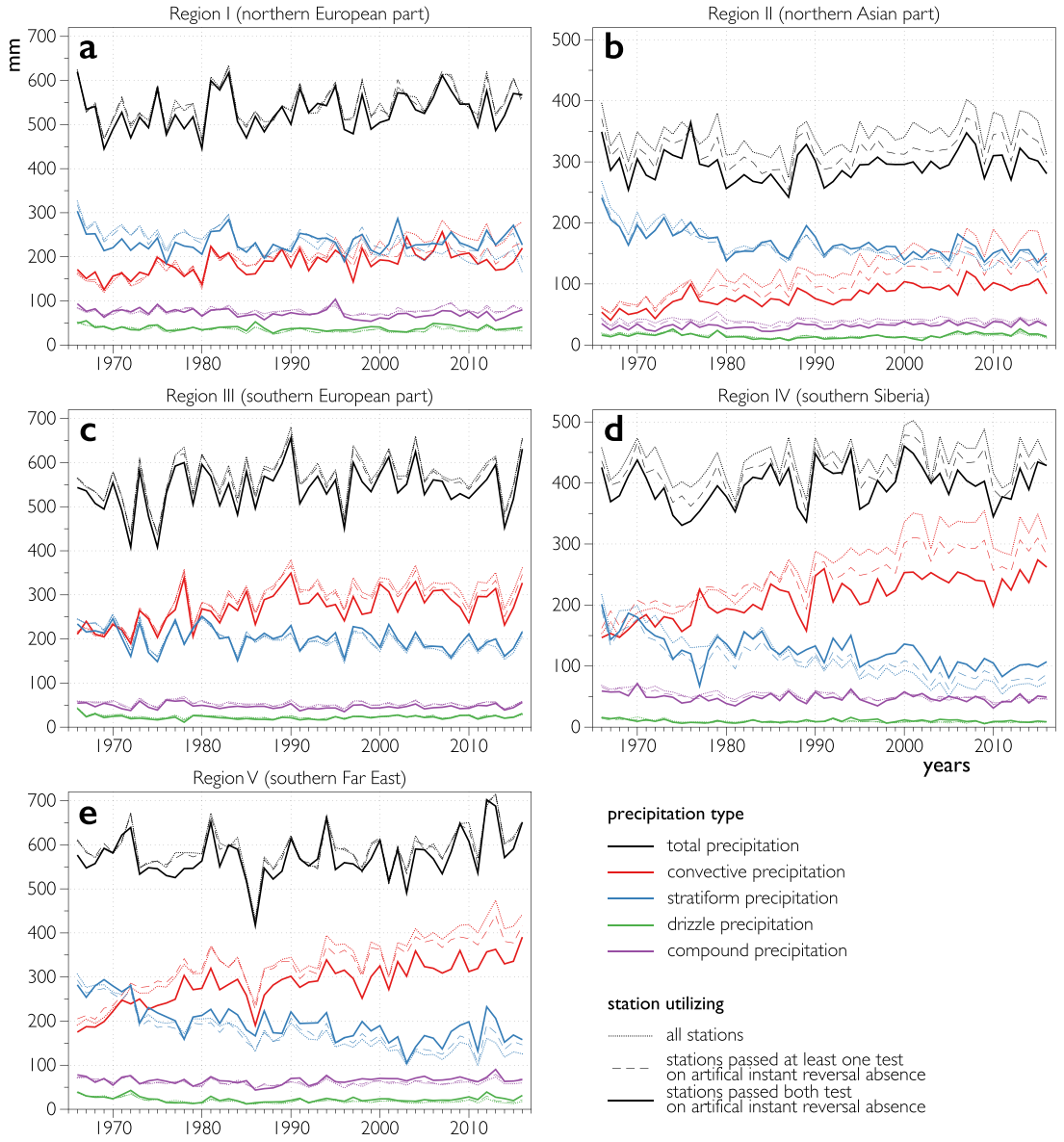

Figure 6. Interannual variations of annual precipitation totals aggregated for five regions (see figure 1 for information on region boundaries). Black, red, blue, green, and magenta colors denote total, convective, stratiform, drizzle, and compound precipitation totals, respectively. Solid (dashed) lines stand for the result of aggregation of stations that passed both tests (only one test) on artificial instant reversal absence; dotted lines display the result of aggregation of all stations.

trends in P_{Conv} and negative trends in P_{Strat}, while the difference between stations that passed one or both tests is less prominent.

Among all regions, the largest trends in the precipitation totals are noted for the south of the Far East (the region V), where P_{Strat} declines from 250–300 mm in the 1960s to 150–200 mm in the 2010s, while P_{Conv} shows the upward change from 200 mm to 300–350 mm during the same period. Note that for all southern regions (the regions III–V) absolute values of P_{Conv} were comparable to those of P_{Strat} in the 1970s but started to prevail from the 1980s. In the northern regions (regions I and II), f_{Strat} is still greater than f_{Conv} but their difference is decreasing. The long-term increase of convective precipitation and decrease of stratiform are in agreement with previously reported decadal changes of cloud type variations (Sun *et al* 2001, Khlebnikova and Sall 2009). The redistribution of the total precipitation between stratiform and convective has no effect on the drizzle and compound precipitation, which both show generally low variability and mostly insignificant trends (figure 6, table 1).

The largest trends of absolute precipitation characteristics (*P*, *P95*, *I*) are noted for most of the regions in the summer (table 2), except for region V, where changes in autumn are also prominent. For relative characteristics (*f*, *R95p*, and *R95pTOT*), changes in spring and autumn are greater than in summer. Convective precipitation characteristics tend to show statistically significant positive trends for all regions and for all seasons except winter (when insignificant trends of both signs are identified, table 2). Instead,

Table 1. Trends of annual precipitation totals (mm/decade) for different regions (see figure 1 for information on region boundaries) and different stations utilized (*all stations*—all stations in region except those that have too many gaps (>5 missing years), are located at high elevation (>1000 m), or have been relocated; *one test passing*—stations that passed only one test on the artificial instant reversal absence; *both tests passing*—stations that passed both tests on the artificial instant reversal absence). Trends are computed with the Theil–Sen estimator. Bold fonts denote statistically significant trends (at a level of 0.05). Significance is obtained with the nonparametric Mann–Kendall test. Numbers of utilized stations are also shown.

Precipitation type	Regions	I	II	III	IV	V
All precipitation	*All stations*	**8.44**	**6.17**	8.64	5.86	7.70
	One test passing	**7.85**	4.38	6.75	4.94	7.24
	Both tests passing	8.05	2.38	5.95	5.10	7.12
Convective precipitation	*All stations*	**24.90**	**23.70**	**22.95**	**39.77**	**41.32**
	One test passing	**14.14**	**15.28**	**18.59**	**24.87**	**31.62**
	Both tests passing	**9.45**	**9.89**	**15.40**	**20.18**	**28.04**
Stratiform precipitation	*All stations*	**−15.55**	**−15.67**	**−11.45**	**−25.58**	**−28.15**
	One test passing	**−6.38**	**−10.79**	**−8.93**	**−15.05**	**−20.54**
	Both tests passing	0.89	**−8.82**	**−6.44**	**−12.30**	**−20.33**
Drizzle precipitation	*All stations*	**−1.98**	**−0.78**	−0.34	**−0.79**	**−1.79**
	One test passing	−0.78	−0.23	0.08	−0.44	−0.80
	Both tests passing	−0.34	0.24	0.37	−0.12	0.18
Compound precipitation	*All stations*	0.57	0.23	**−1.36**	**−3.95**	−0.76
	One test passing	0.44	0.55	−0.94	**−2.51**	0.42
	Both tests passing	**−2.77**	**1.54**	−0.85	−1.50	1.00
Number of stations	*All stations*	*49*	*73*	*121*	*86*	*98*
	One test passing	*36*	*58*	*109*	*54*	*69*
	Both tests passing	*17*	*40*	*57*	*25*	*33*

stratiform precipitation characteristics generally show significant negative trends but with smaller magnitudes however (especially for the regions II and III). Moreover, region I is dominated by positive changes in stratiform precipitation characteristics (*P, I, R95p*) which may be associated with a poleward shift of mid-latitude storm tracks (Mokhov *et al* 2009, Bender *et al* 2012, Eastman and Warren 2013, Tilinina *et al* 2013).

4. Discussion and conclusions

The moderate increase in the total precipitation over NE over the last five decades is accompanied by the tremendous growth of convective precipitation and the concurrent reduction of stratiform precipitation throughout the entire region. In general, rates of convective precipitation increase are greater than those of stratiform precipitation decrease (the latter even shows positive trends, primarily in winter in the northern regions of NE). Generally, convective and stratiform precipitation totals and heavy precipitation sums exhibit major changes in summer, while fractional contributions of these two precipitation types to the total precipitation (including the contribution of heavy precipitation events) show the strongest trends in transition seasons. This singles out spring and autumn as more summer-like seasons in terms of precipitation regime, which is in line with the previous results by Sun *et al* (2001) who found this tendency for cloud types.

Heavy convective precipitation events have started to contribute more to total precipitation. The statistically significant trends amount to 1%–2%/decade for broad regions (resulting in an increase of up to 10% for the last fifty years) being even higher at particular stations (up to 5%/decade). The largest increase is found over the southern Far East region (mostly because of the increase in the intensity of convective precipitation with trends of about 0.4–0.5 mm/day/decade for the entire region and up to 1.4 mm/day/decade for several stations). The obtained trends highlight the changing character of precipitation over NE with the increasing role of heavy showers.

Our results are in agreement with the previous findings that showed the increase of convective precipitation over the Eurasian continent. Particularly, positive trends for showery precipitation were found for central Europe (Rulfová and Kyselý 2014), Northern China (Han *et al* 2016), and Russia (Ye *et al* 2017). Ye *et al* (2017), who restricted their analysis of data up until the year 2000 and used all stations (including those with questionable reports), obtained trends for precipitation totals that are twice as strong as our findings. Such strong trends may result either from using all stations without a discontinuity check or from the analyzed period being shorter. To reveal the main cause of the overestimation, we calculated precipitation trends for the two additional temporal periods: 1966–2000 (the same as in Ye *et al* (2017)) and 2001–2016 (tables S1, S2). For the longer period, the trend slopes get reduced by 2%–10% for convective precipitation (by 35% in region III) and by 5%–25% for stratiform precipitation. The use of only stations passing both tests on artificial change absence results in a considerably stronger decrease in trend slopes (by 30%–60%). Thus, the use of stations with temporally

Table 2. Trends in annual and seasonal precipitation characteristics of convective (C) and stratiform (S) precipitation types for different regions (see figure 1 for information on region boundaries). Only stations that passed both tests on the artificial instant reversal absence were used (number of stations are shown in brackets for each region). Trends are computed with the Theil–Sen estimator. Bold fonts denote statistically significant trends (at 0.05 level). Significance is obtained with the nonparametric Mann–Kendall test.

		I (17)		II (40)		III (57)		IV (25)		V (33)	
Precipitation characteristics	Regions	C	S	C	S	C	S	C	S	C	S
Precipitation totals, P_{Conv} and P_{Strat} (mm/decade)	*Annual*	**9.45**	0.89	**9.89**	**−8.82**	**15.40**	**−6.44**	**20.18**	**−12.30**	**28.04**	**−20.33**
	Winter	−0.05	**3.02**	**0.38**	**−1.76**	**2.49**	1.06	**1.03**	1.46	**1.61**	−0.75
	Spring	**2.10**	−0.10	**1.72**	**−1.23**	**5.10**	−0.79	**4.77**	**−1.64**	**7.14**	**−4.70**
	Summer	**5.68**	−1.96	**4.89**	**−3.18**	3.60	**−3.25**	**9.38**	**−7.23**	**10.19**	**−7.73**
	Autumn	1.00	−0.94	**2.93**	**−1.86**	**3.86**	−1.59	**4.89**	**−3.28**	**8.48**	**−6.35**
Frequency of precipitation events, pP_{Conv} and pP_{Strat} (per decade)	*Annual*	**0.01**	**−0.01**	**0.01**	**−0.01**	**0.01**	**−0.01**	**0.01**	**−0.01**	**0.01**	**−0.01**
	Winter	0.01	0	**0.01**	**−0.02**	**0.01**	0	**0.01**	0	0	0
	Spring	**0.01**	**−0.01**	**0.01**	**−0.01**	**0.01**	**−0.01**	**0.01**	**−0.01**	**0.01**	**−0.01**
	Summer	**0.01**	**−0.01**	**0.01**	**−0.01**	0	**−0.01**	**0.01**	**−0.01**	0	**−0.01**
	Autumn	0	**−0.01**	**0.01**	**−0.01**	**0.01**	**−0.01**	**0.02**	**−0.02**	**0.01**	**−0.01**
Daily precipitation intensity, I_{Conv} and I_{Strat} (mm/day/decade)	*Annual*	**0.05**	**0.06**	**0.11**	−0.01	**0.08**	0.02	**0.09**	**−0.07**	**0.38**	**−0.18**
	Winter	0.03	**0.05**	**0.09**	0	**0.05**	0.05	**0.04**	**0.05**	**0.26**	−0.04
	Spring	**0.06**	**0.08**	**0.12**	0.01	**0.11**	0.06	**0.16**	0.02	**0.40**	**−0.12**
	Summer	**0.10**	**0.26**	**0.15**	0	**0.12**	0.07	**0.16**	−0.01	**0.47**	−0.08
	Autumn	0.02	0.05	**0.11**	−0.01	**0.17**	**0.07**	0.04	**−0.07**	**0.38**	**−0.26**
Fraction of P_{Conv} and P_{Strat} in total precipitation P, f_{Conv} and f_{Strat} (%/decade)	*Annual*	**1.66**	**−0.85**	**2.59**	**−3.10**	**2.25**	**−1.86**	**4.36**	**−3.83**	**3.88**	**−3.86**
	Winter	0.72	0.38	**0.69**	**−0.87**	**1.81**	**−0.95**	**1.52**	**−1.39**	**2.03**	**−2.61**
	Spring	**1.86**	−0.36	**2.92**	**−3.29**	**2.87**	**−2.24**	**5.15**	**−4.48**	**5.47**	**−5.77**
	Summer	**2.06**	**−1.78**	**2.68**	**−3.10**	**1.83**	**−1.94**	**4.64**	**−3.80**	**3.12**	**−3.16**
	Autumn	**1.26**	−0.57	**2.67**	**−3.07**	**2.77**	**−2.66**	**5.73**	**−5.45**	**4.82**	**−4.94**
Precipitation sum obtained during very wet days, $P95_{Conv}$ and $P95_{Strat}$ (mm/decade)	*Annual*	**3.80**	1.29	**3.40**	**−3.61**	**6.72**	−0.89	**7.36**	**−6.13**	**12.04**	**−8.54**
	Winter	−0.20	**1.27**	**0.07**	−0.51	**0.68**	1.07	**0.26**	0.74	**0.72**	−0.11
	Spring	**0.99**	0.68	**0.61**	−0.21	**1.95**	0.06	**2.03**	**−0.63**	**3.34**	**−1.76**
	Summer	**2.52**	−0.07	**1.83**	**−0.97**	**2.48**	**−0.80**	**4.19**	**−1.81**	**5.21**	**−1.60**
	Autumn	0.36	−0.05	**1.08**	−0.57	**2.07**	0.45	**1.61**	**−1.05**	**3.21**	**−2.28**
Contribution of heavy precipitation to precipitation totals, $R95p_{Conv}$ and $R95p_{Strat}$ (%/decade)	*Annual*	**0.90**	**0.83**	**1.05**	**−0.97**	**0.86**	0.10	**1.16**	**−2.71**	**1.81**	**−1.85**
	Winter	0.13	**1.04**	**1.64**	0.03	**1.51**	0.70	0.70	0.95	**1.93**	0.42
	Spring	**2.31**	**1.40**	**1.80**	−0.14	**1.32**	0.35	**3.33**	**−1.72**	**3.70**	**−2.18**
	Summer	**1.61**	0.31	**1.21**	**−1.12**	**0.90**	−0.81	**1.68**	−1.13	**2.12**	**−0.77**
	Autumn	0.38	0.74	**2.65**	−0.51	**2.01**	0.79	**1.58**	**−2.14**	**2.50**	**−1.37**
Contribution of $P95_{Conv}$ and $P95_{Strat}$ to P, $PR95pTOT_{Conv}$ and $R95pTOT_{Strat}$ (%/decade)	*Annual*	**0.73**	0.10	**0.93**	**−1.43**	**0.92**	**−0.35**	**1.52**	**−1.83**	**1.79**	**−1.46**
	Winter	−0.05	**0.89**	**0.12**	−0.12	**0.49**	0.39	**0.33**	0.63	**0.84**	0.16

Table 2. (Continued.)

Precipitation characteristics	Regions	I (17)		II (40)		III (57)		IV (25)		V (33)	
		C	S	C	S	C	S	C	S	C	S
	Spring	**1.13**	**0.78**	**1.02**	−0.51	**1.17**	−0.22	**2.49**	**−1.30**	**2.62**	**−1.64**
	Summer	**1.32**	−0.25	**0.99**	**−1.01**	**1.05**	**−0.50**	**1.95**	**−1.00**	**1.91**	**−0.63**
	Autumn	**0.33**	0.15	**1.08**	**−0.89**	**1.26**	0.14	**1.57**	**−1.51**	**1.81**	**−1.21**

Table 3. Slope of regression of mean seasonal daily intensity of convective (C) and stratiform (S) precipitation to mean seasonal temperature for different regions (see figure 1 for information on region boundaries) (in % $^{\circ}C^{-1}$). Regression slopes are computed with the Theil–Sen estimator. Bold fonts denote statistically significant trends (at a level of 0.05). Significance is obtained with the nonparametric Mann–Kendall test. Only stations that passed both tests on the artificial instant reversal absence are used. Temperature is calculated by simple averaging of seasonal mean temperature for the same stations (since temperature data are missing for several stations for regions I–III, fewer stations are used for these regions; number of used stations is shown in brackets). Percentage of intensity is calculated with respect to 51 years mean of intensity.

Regions	I (16)		II (39)		III (54)		IV (25)		V (33)	
Precipitation type	C	S	C	S	C	S	C	S	C	S
Winter	1.59	1.43	3.45	0.61	2.75	0.71	1.11	−0.32	5.13	−3.03
Spring	**2.66**	1.54	2.36	−0.26	1.02	0.13	1.20	−2.63	**6.18**	**−5.96**
Summer	**4.78**	3.07	**9.76**	−1.15	2.34	1.47	2.81	−0.96	**13.76**	**−8.17**
Autumn	2.98	2.10	4.80	0.78	2.29	2.60	1.48	−2.24	8.20	−3.84

homogeneous time series of weather and cloud types is crucial for estimating robust trends in the convective and stratiform precipitation.

Different causes may determine seasonal and regional patterns of changes in precipitation types. From a thermodynamic perspective, ongoing air temperature increase yields air moisture increase with the rate for saturated vapor pressure at 7% $^{\circ}C^{-1}$ (the so-called Clausius–Clapeyron (CC) rate (Trenberth *et al* 2003)) that suggests a scale for precipitation extreme intensity growth with the warming. For central Europe, for an eight year period, Berg *et al* (2013) found the CC rate of increase of stratiform precipitation extreme intensity with temperature, and the exceedance of this rate for convective extremes. Similar results were obtained for South Korea for a 24-year period (Park and Min 2017). For the long-term view, annual means of convective (stratiform) precipitation intensity increase (decrease) with rising temperature (Ye *et al* 2017). Our results confirm previous findings and show seasonal variation of long-term precipitation response to changing temperature (table 3) with the maximum in summer. A particularly large summer response is found in the southern Far East region where it is close to the so-called super (doubled) CC rate (13.8% $^{\circ}C^{-1}$). Such a high CC rate in this region in summer may be associated with high surface air humidity (figure S7) that is critical for establishing a doubled CC rate (Lenderink *et al* 2017). The vertical structure of temperature and humidity sets a convective instability of the atmosphere, which is an important factor for convective precipitation intensity (Loriaux *et al* 2017). Specifically, characteristics of convective precipitation have a positive statistically significant correlation with the convective available potential energy (CAPE) for most of the stations, while stratiform precipitation is almost uncorrelated with CAPE (figure 7, table S3). Presumably, a large part of the positive trends of convective precipitation in transition seasons is associated with the observed increase of CAPE (Chernokulsky *et al* 2017b); however, this assumption needs more in-depth analysis. In summer, CAPE significantly increases over the European part of Russia (especially near the Black Sea), but decreases over the large part of the Far East (figure S8), and hence plays a smaller role in shaping the observed precipitation trends in this region (table S3). The diversity in the obtained regional responses is linked with the nonlinearity of the temperature–precipitation and instability–precipitation relationships that are determined by atmosphere dynamics and microphysics.

Atmospheric dynamics and microphysics are supposed to be important for the observed redistribution between two types of precipitation over NE. In particular, atmospheric fronts frequency changes (Berry *et al* 2011a), together with changes in the number of extremely strong fronts (Schemm *et al* 2017), may influence the balance between convective and stratiform precipitation. The increase in the frequency of strong fronts in summer (Schemm *et al* 2017) (when cold fronts are prevailing (Berry *et al* 2011b)) may result in an increased role of convective precipitation. The poleward shift of storm tracks (Mokhov *et al* 2009, Bender *et al* 2012, Eastman and Warren 2013), especially pronounced in winter, leads to a decrease in large-scale (stratiform) precipitation in southern regions of NE and to an increase in central and northern regions. This tendency has been confirmed with the presented results that showed an increase in stratiform precipitation in the north and center of the European part of Russia. In line with this, while the transportation of atmospheric moisture in Northern Eurasia does not show significant trends, the relative contribution of the transient eddies does show a significant increase from 1979 onwards (Dufour *et al* 2016). Regional and local processes may also play a role. Specifically, the increasing intensity of the Siberian High leads to a decline in stratiform clouds and associated precipitation in the south of NE in winter (Chernokulsky *et al* 2013). Near the Black Sea, sea surface temperature warming leads to tropical-like convection development (enhanced by orography) that yields heavy and devastating showers (Meredith *et al* 2015a, 2015b). At the western Arctic coast, convective precipitation may have positive trends in the cold part of a year associated with intensified cold air outbreaks (and the consequent development of convection) due to sea-ice retreat (Esau and Chernokulsky 2015).

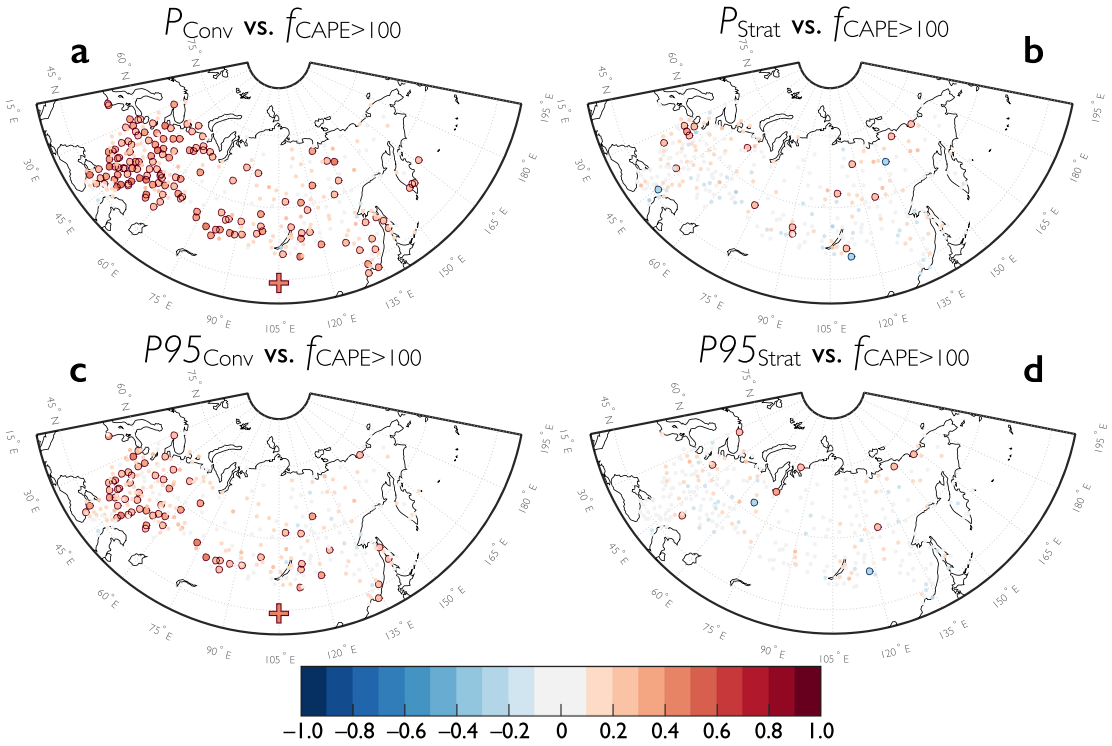

Figure 7. Mann–Kendall correlation coefficient between detrended time series of summer P_{Conv} (a), P_{Strat} (b), $P95_{Conv}$ (c), $P95_{Strat}$ (d), and frequency of CAPE $>$ 100 J kg^{-1} in summer (from ERA-Interim data (Dee *et al* 2011) that is calculated for the reanalysis grid boxes that include the meteorological station locations) for the 1979–2016 period. Coefficients are shown only for the 326 stations that passed at least one of the tests on artificial instant reversal absence.

Tropospheric aerosols may also have regional effects since they diversely influence convective and stratiform precipitation (Tao *et al* 2012). Ongoing variations in aerosol properties (see e.g. Chin *et al* 2014, Zhao *et al* 2017) may alter precipitation characteristics, especially over polluted regions like the south of the Far East (Kinne *et al* 2013) where the largest trends in convective precipitation are found.

The observed change in NE precipitation structure is an important regional consequence of global climate change that may influence the regional water cycle. Redistribution of total precipitation between convective and stratiform types is likely a result of a delicate balance among various causes including thermodynamics, dynamics, and microphysics. Further analysis based on various observations (surface, weather radars, satellites) and specially conducted model simulations is needed to disentangle the role of individual drivers in the discovered precipitation redistribution in order to attribute the revealed tendencies to climate change and internal climate variability.

Acknowledgments

This paper is dedicated to the memory of Dr Olga Bulygina, our deeply esteemed colleague and an ardent scientist. She largely contributed to this paper before she passed away in early 2018. She will be dearly missed. The study has been supported by the Russian Science Foundation (project no. 18-77-10076). Station data have been processed under the RFBR 17-29-05098 project. Support for OZ from the Agence Nationale de la Recherché through the ARCTIC-ERA project is appreciated. The authors are grateful to the editor and two anonymous reviewers for their helpful comments on the manuscript.

ORCID iDs

Alexander Chernokulsky https://orcid.org/0000-0003-3635-6263

References

Ahmed F and Schumacher C 2015 Convective and stratiform components of the precipitation-moisture relationship *Geophys. Res. Lett.* **42** 10453–62

Alibegova Z D 1985 *Spatio-temporal Structure of Liquid Precipitation* (Moscow: Gidrometeoizdat) (in Russian)

Anagnostou E N 2006 A convective/stratiform precipitation classification algorithm for volume scanning weather radar observations *Met. Apps* **11** 291–300

Bender F A-M, Ramanathan V and Tselioudis G 2012 Changes in extratropical storm track cloudiness 1983–2008: observational support for a poleward shift *Clim. Dyn.* **38** 2037–53

Berry G, Jakob C and Reeder M 2011a Recent global trends in atmospheric fronts *Geophys. Res. Lett.* **38** L21812

Berry G, Reeder M J and Jakob C 2011b A global climatology of atmospheric fronts *Geophys. Res. Lett.* **38** L04809

Berg P, Moseley C and Haerter J O 2013 Strong increase in convective precipitation in response to higher temperatures *Nature Geosci.* **6** 181–5

Bogdanova E G, Gavrilova S Y and Il'in B M 2010 Time changes of atmospheric precipitation in Russia from the corrected data during 1936–2000 *Russ. Meteorol. Hydro.* **35** 706–14

Bulygina O N, Bulygina O N, Veselov V M, Veselov V M, Razuvaev V N, Razuvaev V N, Aleksandrova T M and Aleksandrova T M 2014 Description of the dataset of observational data on major meteorological parameters from Russian weather stations (http://meteo.ru/data/163-basic-parameters)

Chernokulsky A V, Bulygina O N and Mokhov I I 2011 Recent variations of cloudiness over Russia from surface daytime observations *Environ. Res. Lett.* **6** 035202

Chernokulsky A, Mokhov I I and Nikitina N 2013 Winter cloudiness variability over Northern Eurasia related to the siberian high during 1966–2010 *Environ. Res. Lett.* **8** 045012

Chernokulsky A V, Esau I, Bulygina O N, Davy R, Mokhov I I, Outten S and Semenov V A 2017a Climatology and interannual variability of cloudiness in the Atlantic Arctic from surface observations since the late nineteenth century *J. Clim.* **30** 2103–20

Chernokulsky A V, Kurgansky M V and Mokhov I I 2017b Analysis of changes in tornadogenesis conditions over Northern Eurasia based on a simple index of atmospheric convective instability *Dokl. Earth Sci.* **477** 1504–9

Chernokulsky A V, Kozlov F A, Zolina O G, Bulygina O N and Semenov V A 2018 Climatology of precipitation of different genesis in Northern Eurasia *Russ. Meteorol. Hydro.* **43** 425–35

Chin M *et al* 2014 Multi-decadal aerosol variations from 1980–2009: a perspective from observations and a global model *Atmos. Chem. Phys.* **14** 3657–90

Collins M *et al* 2018 Challenges and opportunities for improved understanding of regional climate dynamics *Nature Clim. Change* **8** 101–8

Dai A 2001 Global precipitation and thunderstorm frequencies. Part I: seasonal and interannual variations *J. Clim.* **14** 1092–111

Dee D P *et al* 2011 The ERA-interim reanalysis: configuration and performance of the data assimilation system *Q. J. R. Meteorol. Soc.* **137** 553–97

Donat M G, Lowry A L, Alexander L V, O'Gorman P A and Maher N 2016 More extreme precipitation in the world's dry and wet regions *Nature Clim. Change.* **6** 508–513

Dufour A, Zolina O and Gulev S K 2016 Atmospheric moisture transport to the Arctic: assessment of reanalyses and analysis of transport components *J. Clim.* **29** 5061–81

Eastman R and Warren S G 2013 A 39-yr survey of cloud changes from land stations worldwide 1971–2009: long-term trends, relation to aerosols, and expansion of the tropical belt *J. Clim.* **26** 1286–303

Esau I N and Chernokulsky A V 2015 Convective cloud fields in the Atlantic sector of the Arctic: satellite and ground-based observations *Izv. Atmos. Ocean. Phys.* **51** 1007–20

Evseev P K 1958 Distribution of showery and nonshowery precipitation on the territory of the USSR *Sov. Meteorol. Gidrol.* **3** 15–20 (in Russian)

Groisman P Y *et al* 1999 Changes in the probability of heavy precipitation: important indicators of climatic change *Clim. Change* **42** 243–83

Groisman P Y, Knight R W, Easterling D R, Karl T R, Hegerl G C and Razuvaev V N 2005 Trends in intense precipitation in the climate record *J. Clim.* **18** 1326–50

Groisman P Y, Bogdanova E G, Alexeev V A, Cherry J E and Bulygina O N 2014 Impact of snowfall measurement deficiencies on quantification of precipitation and its trends over Northern Eurasia *Led i Sneg* **2** 29–43

Groisman P *et al* 2017 Northern eurasia future initiative (NEFI): facing the challenges and pathways of global change in the twenty-first century *Prog. Earth Planet. Sci.* **4** 1–48

Han X, Xue H, Zhao C and Lu D 2016 The roles of convective and stratiform precipitation in the observed precipitation trends in Northwest China during 1961–2000 *Atmos. Res.* **169** 139–46

Houze R A Jr 1997 Stratiform precipitation in regions of convection: a meteorological paradox? *Bull. Am. Meteorol. Soc.* **78** 2179–96

Khlebnikova E I and Sall I A 2009 Peculiarities of climatic changes in cloud cover over the Russian Federation *Russ. Meteorol. Hydro.* **34** 411–7

Khon V C, Mokhov I I, Roeckner E and Semenov V A 2007 Regional changes of precipitation characteristics in Northern Eurasia from simulations with global climate model *Glob. Planet. Change* **57** 118–23

Kinne S, O'Donnel D, Stier P, Kloster S, Zhang K, Schmidt H, Rast S, Giorgetta M, Eck T F and Stevens B 2013 MAC-v1: a new global aerosol climatology for climate studies *J. Adv. Model. Earth Syst.* **5** 704–40

Klein Tank A M G and Konnen G P 2003 Trends in indices of daily temperature and precipitation extremes in Europe, 1946–99 *J. Clim.* **16** 3665–80

Kurgansky M V, Chernokulsky A V and Mokhov I I 2013 The tornado over Khanty-Mansiysk: an exception or a symptom? *Russ. Meteorol. Hydro.* **38** 539–46

Leander R, Buishand T A and Tank A M G K 2014 An alternative index for the contribution of precipitation on very wet days to the total precipitation *J. Clim.* **27** 1365–78

Lenderink G, Barbero R and Loriaux J M 2017 Super Clausius–Clapeyron scaling of extreme hourly convective precipitation and its relation to large-scale atmospheric conditions *J. Clim.* **30** 6037–52

Livezey R E and Chen W Y 1983 Statistical field significance and its determination by Monte Carlo techniques *Mon. Weather Rev.* **111** 46–59

Loriaux J M, Lenderink G and Siebesma A P 2017 Large-scale controls on extreme precipitation *J. Clim.* **30** 955–68

Marsh P T, Brooks H E and Karoly D J 2009 Preliminary investigation into the severe thunderstorm environment of Europe simulated by the Community Climate System Model 3 *Atmos. Res.* **93** 607–18

Meredith E P, Maraun D, Semenov V A and Park W 2015a Evidence for added value of convection-permitting models for studying changes in extreme precipitation *J. Geophys. Res.: Atmos.* **120** 12500–13

Meredith E P, Semenov V A, Maraun D, Park W and Chernokulsky A V 2015b Crucial role of black sea warming in amplifying the 2012 Krymsk precipitation extreme *Nature Geosci.* **8** 615–9

Milly P C D, Dunne K A and Vecchia A V 2005 Global pattern of trends in streamflow and water availability in a changing climate *Nature* **438** 347–50

Mokhov I I, Semenov V A and Khon V C 2003 Estimates of possible regional hydrologic regime changes in the 21st century based on global climate models *Izv. Atmos. Ocean. Phys.* **39** 130–44

Mokhov I I, Roekner E, Semenov V A and Khon V C 2005 Extreme precipitation regimes in Northern Eurasia in the 20th century and their possible changes in the 21st century *Dokl. Earth Sci.* **403** 767–70

Mokhov I I and Akperov M G 2006 Tropospheric lapse rate and its relation to surface temperature from reanalysis data *Izv. Atmos. Ocean. Phys.* **42** 430–8

Mokhov I I, Chernokul'skii A V, Akperov M G, Dufresne J-L and Le Treut H 2009 Variations in the characteristics of cyclonic activity and cloudiness in the atmosphere of extratropical latitudes of the Northern hemisphere based from model calculations compared with the data of the reanalysis and satellite data *Dokl. Earth Sci.* **424** 147–50

Mokhov I I 2014 Hydrological anomalies and tendencies of change in the basin of the Amur River under global warming *Dokl. Earth Sci.* **455** 459–62

Mokhov I I and Semenov V A 2016 Weather and climate anomalies in Russian regions related to global climate change *Russ. Meteorol. Hydro.* **41** 84–92

Park I-H and Min S-K 2017 Role of convective precipitation in the relationship between subdaily extreme precipitation and temperature *J. Clim.* **30** 9527–37

Peleg N, Marra F, Fatichi S, Molnar P, Morin E, Sharma A and Burlando P 2018 Intensification of convective rain cells at warmer temperatures observed from high-resolution weather radar data *J. Hydrometeor.* **19** 715–26

Pistotnik G, Groenemeijer P and Sausen R 2017 Validation of convective parameters in MPI-ESM decadal hindcasts (1971–2012) against ERA-interim reanalyses *Meteorol. Z.* **25** 753–66

Púčik T, Groenemeijer P, Rädler A T, Tijssen L, Nikulin G, Prein A F, van Meijgaard E, Fealy R, Jacob D and Teichmann C 2017 Future changes in European severe convection environments in a regional climate model ensemble *J. Clim.* **30** 6771–94

Riemann-Campe K, Fraedrich K and Lunkeit F 2009 Global climatology of convective available potential energy (CAPE) and convective inhibition (CIN) in ERA-40 reanalysis *Atmos. Res.* **93** 534–45

Ruiz-Leo A M, Hernández E, Queralt S and Maqueda G 2013 Convective and stratiform precipitation trends in the Spanish Mediterranean coast *Atmos. Res.* **119** 46–55

Rulfová Z and Kyselý J 2013 Disaggregating convective and stratiform precipitation from station weather data *Atmos. Res.* **134** 100–15

Rulfová Z and Kyselý J 2014 Trends of convective and stratiform precipitation in the Czech Republic, 1982–2010 *Adv. Meteorol.* **2014** 647938

Schär C *et al* 2016 Percentile indices for assessing changes in heavy precipitation events *Clim. Change* **137** 201–16

Schemm S, Sprenger M, Martius O, Wernli H and Zimmer M 2017 Increase in the number of extremely strong fronts over Europe? A study based on ERA-interim reanalysis (1979–2014) *Geophys. Res. Lett.* **44** 553–61

Semenov V A and Bengtsson L 2002 Secular trends in daily precipitation characteristics: greenhouse gas simulation with a coupled AOGCM *Clim. Dyn.* **19** 123–40

Sempere-Torres D, Sanchez-Diezma R, Zawadski I and Creutin J D 2000 Identification of stratiform and convective areas using radar data with application to the improvement of DSD analysis and Z-R relations *Phys. Chem. Earth B: Hydrol. Ocean. Atmos.* **25** 985–90

Shkolnik I, Pavlova T, Efimov S and Zhuravlev S 2018 Future changes in peak river flows across northern Eurasia as inferred from an ensemble of regional climate projections under the IPCC RCP8.5 scenario *Clim. Dyn.* **50** 215–30

Steiner M and Smith J A 1998 Convective versus stratiform rainfall: an ice-microphysical and kinematic conceptual model *Atmos. Res.* **47–48** 317–26

Sui C-H, Tsay C-T and Li X 2007 Convective–stratiform rainfall separation by cloud content *J. Geophys. Res.* **112** 30

Sun B, Groisman P Y and Mokhov I I 2001 Recent changes in cloud-type frequency and inferred increases in convection over the United States and the former USSR *J. Clim.* **14** 1864–80

Tao W-K, Chen J-P, Li Z, Wang C and Zhang C 2012 Impact of aerosols on convective clouds and precipitation *Rev. Geophys.* **50** RG2001

Taszarek M, Brooks H E, Czernecki B, Szuster P and Fortuniak K 2018 Climatological aspects of convective parameters over Europe: a comparison of ERA-interim and sounding data *J. Clim.* **31** 4281–308

Tilinina N, Gulev S K, Rudeva I and Koltermann P 2013 Comparing cyclone life cycle characteristics and their interannual variability in different reanalyses *J. Clim.* **26** 6419–38

Tremblay A 2005 The stratiform and convective components of surface precipitation *J. Atmos. Sci.* **62** 1513–28

Trenberth K E, Dai A, Rasmussen R M and Parsons D B 2003 The changing character of precipitation *Bull. Am. Meteorol. Soc.* **84** 1205–18

Xu S, Lin W and Sui C H 2013 The separation of convective and stratiform precipitation regions of simulated typhoon Chanchu and its sensitivity to the number concentration of cloud droplets *Atmos. Res.* **122** 229–36

Yang Y, Chen X and Qi Y 2013 Classification of convective/stratiform echoes in radar reflectivity observations using a fuzzy logic algorithm *J. Geophys. Res.* **118** 1896–905

Ye H, Fetzer E J, Wong S and Behrangi A 2015 Increasing atmospheric water vapor and higher daily precipitation intensity over northern Eurasia *Geophys. Res. Lett.* **42** 9404–10

Ye H, Fetzer E J, Wong S, Lambrigtsen B H, Wong T, Chen L and Van Dang 2016 More frequent showers and thunderstorm days under a warming climate: evidence observed over Northern Eurasia from 1966–2000 *Clim. Dyn.* **49** 1933–44

Ye H, Fetzer E J, Wong S and Lambrigtson B H 2017 Rapid decadal convective precipitation increase over Eurasia during the last three decades of the 20th century *Sci. Adv.* **3** e1600944

Ye H 2018 Changes in duration of dry and wet spells associated with air temperatures in Russia *Environ. Res. Lett.* **13** 034036

Zhao B, Jiang J H, Gu Y, Diner D, Worden J, Liou K-N, Su H, Xing J, Garay M and Huang L 2017 Decadal-scale trends in regional aerosol particle properties and their linkage to emission changes *Environ. Res. Lett.* **12** 054021

Zolina O, Simmer C, Belyaev K, Kapala A and Gulev S 2009 Improving estimates of heavy and extreme precipitation using daily records from european rain gauges *J. Hydrometeor.* **10** 701–16

Zolina O, Simmer C, Gulev S K and Kollet S 2010 Changing structure of European precipitation: longer wet periods leading to more abundant rainfalls *Geophys. Res. Lett.* **37** L06704

Zolina O, Simmer C, Belyaev K, Gulev S K and Koltermann P 2013 Changes in the duration of European wet and dry spells during the last 60 years *J. Clim.* **26** 2022–47

Zolina O G and Bulygina O N 2016 Current climatic variability of extreme precipitation in Russia *Fund. App. Clim.* **1** 84–103 (in Russian)